

Voronoi Progressive Widening: Efficient Online Solvers for Continuous Space MDPs and POMDPs with Provably Optimal Components

Michael H. Lim,¹ Claire J. Tomlin,² Zachary N. Sunberg³

¹ University of California, Berkeley, Department of Statistics, 367 Evans Hall, Berkeley, CA 94720

² University of California, Berkeley, Department of EECS, 626 Hearst Ave, Berkeley, CA 94720

³ University of Colorado Boulder, Department of Aerospace Engineering Sciences, 3775 Discovery Drive, Boulder, CO 80303
michaelhlim@berkeley.edu, tomlin@eecs.berkeley.edu, zachary.sunberg@colorado.edu

Abstract

Markov decision processes (MDPs) and partially observable MDPs (POMDPs) can effectively represent complex real-world decision and control problems. However, continuous space MDPs and POMDPs, i.e. those having continuous state, action and observation spaces, are extremely difficult to solve, and there are few online algorithms with convergence guarantees. This paper introduces Voronoi Progressive Widening (VPW), a general technique to modify tree search algorithms to effectively handle continuous or hybrid action spaces, and proposes and evaluates three continuous space solvers: VOSS, VOWSS, and VOMCPOW. VOSS and VOWSS are theoretical tools based on sparse sampling and Voronoi optimistic optimization designed to justify VPW-based online solvers. While previous algorithms have enjoyed convergence guarantees for problems with continuous state and observation spaces, VOWSS is the first with global convergence guarantees for problems that additionally have continuous action spaces. VOMCPOW is a versatile and efficient VPW-based algorithm that consistently outperforms POMCPOW and BOMCP in several simulation experiments.

1 Introduction

The Markov decision process (MDP) and partially observable Markov decision process (POMDP) are flexible mathematical frameworks for expressing stochastic sequential decision problems. MDPs and POMDPs can represent a wide range of real world problems, such as autonomous driving (Bai et al. 2015; Sunberg, Ho, and Kochenderfer 2017), cancer screening (Ayer, Alagoz, and Stout 2012), spoken dialog systems (Young et al. 2013), and aircraft collision avoidance system that will be deployed worldwide (Holland, Kochenderfer, and Olson 2013).

MDP and POMDP are optimization problems in which we aim to find a policy that maps states to actions, which will control the state to maximize the sum of expected rewards. Optimizing in this policy space is computationally demanding, especially in the case of POMDPs because of the uncertainty introduced by imperfect observations (Papadimitriou and Tsitsiklis 1987). One of the most popular ways to effectively deal with this computational challenge is approximate online tree search (Silver and Veness 2010; Ye et al. 2017;

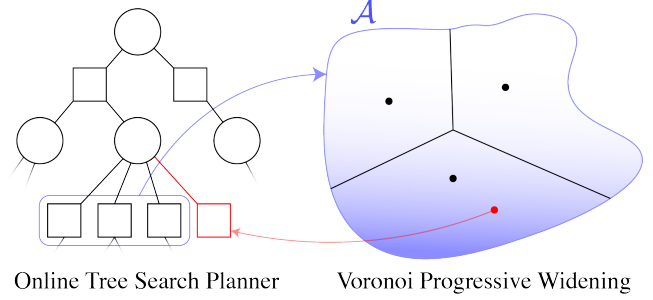


Figure 1: Voronoi progressive widening (VPW) guides the selection of actions to widen the search tree. Circles denote state/belief nodes, squares denote action nodes.

Sunberg, Ho, and Kochenderfer 2017; Kurniawati and Yadav 2016). *Online* algorithms, often based on Monte Carlo Tree Search (MCTS), look for local approximate policies as the agent interacts with the environment rather than computing a global policy that maps every possible outcome to a corresponding action.

While many of these MCTS methods can handle MDPs and POMDPs with large discrete or continuous state or observation spaces with relative ease, they often perform poorly on problems that additionally have large or continuous action spaces (Browne et al. 2012). For instance, since solvers such as POMCP (Silver and Veness 2010) for POMDPs often rely on branching to handle large state space, they tend to excessively branch out the tree for problems with both large state and action spaces. This leads to very shallow trees with poor value function estimates, and even convergence to suboptimal solutions in some cases (Sunberg and Kochenderfer 2018).

Progressive widening (PW) proposed by Couëtoux et al. (2011) addresses this problem by limiting the tree action width by dynamically switching between resampling from a subset of available actions and randomly sampling new actions. However, since the random sampling step in PW is often specified to pick uniformly from the entire action space, it does not fully take advantage of the available Q -value estimates to determine which regions of the action space are more promising to explore.

In this work, we propose Voronoi Progressive Widening (VPW), which

Solver	Problem	Source	Brief Description
VOOT	MDP	Kim et al. (2020)	VOO for deterministic MDPs; optimality guarantees; practical
VOSS	MDP	New	Sparse sampling and VOO; optimality guarantees
VOWSS	POMDP	New	Extends POWSS and VOO; optimality guarantees
POMCPOW	POMDP	Sunberg and Kochenderfer (2018)	Combines POMCP and DPW; practical
VOMCPOW	POMDP	New	POMCPOW using VPW; practical
BOMCP	POMDP	Mern et al. (2021b)	POMCPOW with Gaussian processes; practical

Table 1: Summary of continuous space MDP and POMDP solvers studied and newly proposed in this paper.

ing (VPW), a general technique to modify tree search algorithms to effectively handle continuous or hybrid action spaces. VPW combines principles from Voronoi optimistic optimization (VOO) (Kim et al. 2020) and PW to efficiently branch the tree through random action sampling without relying on any additional prior information or expert knowledge. Furthermore, VPW does not require significant additional computation time to improve the performances of MCTS solvers, and it can handle both continuous and hybrid action spaces with relative ease.

In order to analyze both theoretical and practical implications of VPW, we propose and evaluate three continuous space solvers: VOSS, VOWSS, and VOMCPOW. Here, we define continuous space MDPs and POMDPs to mean those with continuous state, action and observation spaces. Voronoi Optimistic Sparse Sampling (VOSS) and Voronoi Optimistic Weighted Sparse Sampling (VOWSS) are theoretical tools based on sparse sampling (Kearns, Mansour, and Ng 2002), partially observable weighted sparse sampling (POWSS) (Lim, Tomlin, and Sunberg 2020) and VOO designed to justify VPW-based online solvers. While previous algorithms such as POWSS have enjoyed convergence guarantees for problems with continuous state and observation spaces, VOWSS is the first with global convergence guarantees for problems that additionally have continuous action spaces. Finally, Voronoi Optimistic Monte Carlo Planning with Observation Weighting (VOMCPOW) is a versatile and efficient VPW-based algorithm that consistently outperforms state-of-the-art continuous space POMDP solvers POMCPOW (Sunberg and Kochenderfer 2018) and BOMCP (Mern et al. 2021b) in several simulation experiments. Table 1 summarizes the solvers that are extensively discussed and studied in this paper.

The remainder of this paper proceeds as follows: First, Sections 2 and 3 review preliminary definitions and previous work. Then, Section 4 presents an overview of the VOSS and VOWSS algorithms and their theoretical guarantees. Section 5 introduces the VPW algorithm, and describes its strengths as well as how to efficiently implement it in practice. Finally, Section 6 empirically shows the optimality of VOWSS action selection and the efficiency and robustness of VOMCPOW over three different simulation experiments.

2 Preliminaries

MDP and POMDP Formulation A POMDP is defined by a 7-tuple $(\mathcal{S}, \mathcal{A}, \mathcal{O}, \mathcal{T}, \mathcal{Z}, R, \gamma)$: \mathcal{S} is the state space, \mathcal{A} is the action space, \mathcal{O} is the observation space, \mathcal{T} is the

transition density $\mathcal{T}(s'|s, a)$, \mathcal{Z} is the observation density $\mathcal{Z}(o|a, s')$, R is the reward function, and $\gamma \in [0, 1)$ is the discount factor (Kochenderfer 2015; Bertsekas 2005). Similarly, an MDP is defined by a 5-tuple $(\mathcal{S}, \mathcal{A}, \mathcal{T}, R, \gamma)$ with same variable definitions. For POMDPs, since agent receives only observations, the agent can infer the state by maintaining a belief b_t at each step t and updating it with new action and observation pair (a_{t+1}, o_{t+1}) via Bayesian updates (Kaelbling, Littman, and Cassandra 1998). A policy, denoted with π , maps states s_t or beliefs b_t to actions a_t . Thus, to maximize the expected cumulative reward in MDPs and POMDPs, the agent seeks to find the optimal policy π^* .

For simplicity, in the theoretical portion of this paper, we focus on problems with a finite horizon length D , though the basic concepts empirically work well in the infinite horizon case. The state value function V and action value function Q for a given belief b and policy π at step t by Bellman updates for $t \in [0, D-1]$ are defined as follows, where bao indicates the belief b updated with (a, o) :

$$V_t^\pi(b) = \mathbb{E} \left[\sum_{i=t}^{D-1} \gamma^{i-t} R(s_i, \pi(s_i)) \middle| b \right], \quad V_D^\pi(b) = 0 \quad (1)$$

$$Q_t^\pi(b, a) = \mathbb{E} [R(s, a) + \gamma V_{t+1}^\pi(bao) | b] \quad (2)$$

Specifically, the optimal value functions at each depth t should satisfy the following:

$$V_t^*(b) = \max_{a \in \mathcal{A}} Q_t^*(b, a) \quad (3)$$

$$\pi_t^*(b) = \arg \max_{a \in \mathcal{A}} Q_t^*(b, a) \quad (4)$$

$$Q_t^*(b, a) = \mathbb{E} [R(s, a) + \gamma V_{t+1}^*(bao) | b] \quad (5)$$

The formalism can be applied to MDPs in a similar fashion, where we can directly reason about the state s instead of the belief b , and the next step state s' from (s, a) instead of the updated belief bao .

Generative models For many problems cast as MDPs or POMDPs, the probability densities \mathcal{T} and \mathcal{Z} may be difficult to determine explicitly. Thus, some approaches only require that samples are generated with the correct probability. With this requirement, we assume we have access to a generative model G that implicitly defines \mathcal{T}, \mathcal{Z} by generating a new state, s' , reward, r , and observation, o , for POMDPs, given the current state s and action a .

3 Additional Related Work

In addition to the work mentioned in the introduction, there has been much work in solving continuous action MDPs

and POMDPs with online tree search techniques. Several of these techniques build upon double progressive widening (DPW) (Couëtoux et al. 2011), originally designed to solve continuous space MDPs. Most notably, POMCPOW and PFT-DPW (Sunberg and Kochenderfer 2018) extend POMCP and DPW to handle continuous space POMDPs. However, these algorithms use DPW as it is proposed with the inefficient action progressive widening, and can still struggle to solve large scale continuous space POMDPs.

One effective direction to handle continuous action spaces has been to use continuous bandits to sample new actions. Particularly, hierarchical optimistic optimization (HOO) and the corresponding HOOT algorithm (Mansley, Weinstein, and Littman 2011) are at the forefront of these continuous bandit algorithms applied to MCTS. This is followed by works such as HOLOP (Weinstein and Littman 2012) that plans with open-loop trajectories instead of individual actions using HOO, POLY-HOOT (Mao et al. 2020) with polynomial guarantees, and VOO and VOOT (Kim et al. 2020) that we analyze further in this work.

Another direction is to use Bayesian optimization to efficiently sample new actions. CBTS (Morere, Marchant, and Ramos 2016) uses Gaussian processes (GP) to tackle the random action sampling problem. However, CBTS does not use progressive widening approach and uses a separate GP at each belief node, which limits its optimization scope and branching capabilities. Most recently, BOMCP proposed by Mern et al. (2021b) extends POMCPOW by posing the random action sampling step of DPW as a Bayesian optimization problem over all the belief and action nodes. Despite the effectiveness of BOMCP, GPs are very computationally expensive to fit especially over the joint belief and action space, and BOMCP trades off computation time for sample efficiency compared to POMCPOW.

Other directions include GPS-ABT (Seiler, Kurniawati, and Singh 2015) that uses generalized pattern search, PA-POMCPOW that incorporates additional knowledge using score functions (Mern et al. 2021a), and VG-UCT that calculates gradient of the value function (Lee et al. 2020).

4 Online Solvers for Continuous Space MDP and POMDP with Guarantees

We introduce Voronoi Optimistic Sparse Sampling (VOSS) and Voronoi Optimistic Weighted Sparse Sampling (VOWSS), which are continuous space online MDP and POMDP solvers, respectively. VOSS and VOWSS build upon principles from sparse sampling, POWSS and VOO, and thus have global convergence guarantees to the optimal policy. Consequently, VOSS and VOWSS justify the usage of VPW-based solvers that use techniques based on sparse sampling, particle weighting and VOO, such as the VOMCPOW algorithm we introduce in Section 5.

4.1 Algorithms

We define the algorithmic elements shared by VOSS and VOWSS: VOO in Algorithm 1, and SELECTACTION and ESTIMATEV in Algorithm 2. Since the basic principles for

Algorithm 1 VOO Agent (Kim et al. 2020)

Algorithm: $\text{VOO}([s/\bar{b}], q, \omega, \mathcal{D}(\cdot, \cdot), n, d)$

Input: State s or belief particle set \bar{b} , array of function values and their evaluation points $q \equiv \{q([s/\bar{b}], a_i)\}_{i=1}^n$, VOO exploration parameter ω , metric on the action space $\mathcal{D}(\cdot, \cdot)$, iteration number n , depth d .

Output: Updated q , an action a^* .

- 1: Sample a random number $u \sim \text{Unif}[0, 1]$.
- 2: If $u \leq \omega$ or $n = 1$, sample $a \sim \text{Unif}(\mathcal{A})$
- 3: Otherwise, sample $a \sim \text{BestVoronoiCell}(\mathcal{A}, q)$
- 4: Estimate Q_n and insert it to q :

$$\hat{Q}_d([s/\bar{b}], a_n) = \text{ESTIMATEQ}([s/\bar{b}], a_n, d)$$

- 5: Return the updated q and the best action a^* among samples:

$$q = \{q([s/\bar{b}], a_i)\}_{i=1}^n, a^* = \arg \max_{i=1, \dots, n} \{q([s/\bar{b}], a_i)\}$$

VOSS and VOWSS are the same, we denote that the subroutines should either accept a state input s for VOSS or a belief particle set input \bar{b} for VOWSS through the notation $[s/\bar{b}]$. The belief particle set \bar{b} contains pairs (s_i, w_i) that correspond to the generated sample and its corresponding likelihood weight.

VOO is the VOO algorithm from Kim et al. (2020) adapted to our formalism, which searches the action space either uniformly with probability ω or from the best Voronoi cell with probability $1 - \omega$. A Voronoi cell is defined by the set of points closest to the corresponding Voronoi center compared to the other centers, and the best Voronoi cell is the Voronoi cell defined by the Voronoi center with the highest function value. Since Voronoi cells are solely defined by distances to Voronoi centers, VOO additionally takes in a distance metric $\mathcal{D}(\cdot, \cdot)$ as an input, and scales well to higher dimensions unlike HOO.

SELECTACTION is the entry point of the algorithm, which selects the best action for a state or belief $[s/\bar{b}]$ according to the Q -function by recursively calling ESTIMATEQ. ESTIMATEV is a subroutine that returns the value function, V , for an estimated state or belief, by calling ESTIMATEQ for each action and returning the maximum. For VOWSS, the weight at initial step is uniformly normalized to $1/C$, as the samples are drawn directly from b_0 . We omit the fixed global variables/functions $\omega, \mathcal{D}(\cdot, \cdot), \gamma, G, C_s, C_a, D$ in the subsequent recursive calls for convenience. The algorithms in this section are written in a style closer to a plain English format in order to enhance the readability of mathematical machinery used for these algorithms, since VOSS and VOWSS are more theoretical in nature.

We define ESTIMATEQ functions in Algorithm 3 for VOSS and VOWSS, where both methods perform sampling and recursive calls to ESTIMATEV to estimate the Q -function at a given step. Each of the ESTIMATEQ functions follow the same subroutines from each of sparse sampling for VOSS, and POWSS for VOWSS. VOSS simply returns the naive average of the Q -functions calculated via

Algorithm 2 Common Algorithms for VOSS and VOWSS

Algorithm: SELECTACTION($[s_0/b_0], \gamma, G, C_s, C_a, D, \omega$)
Input: Initial state s_0 or belief distribution b_0 , discount γ , generative model G , state width C_s , action width C_a , max depth D , VOO exploration parameter ω .
Output: An action a^* .

- 1: For VOWSS, sample C number of particles from b_0 , initialize weights to $w_i = 1/C$, insert state-weight pairs to belief particle set \bar{b}_0
- 2: For $i = 1, \dots, C_a$, run VOO($[s_0/\bar{b}_0], q_0, i, 0$) with ESTIMATEQ($[s/\bar{b}], a, 0$) to obtain $\{q_0([s_0/\bar{b}_0], a_i)\}_{i=1}^{C_a}$
- 3: Return the best action among samples:

$$a^* = \arg \max_{i=1, \dots, C_a} \{q_0([s_0/\bar{b}_0], a_i)\}$$

Algorithm: ESTIMATEV($[s/\bar{b}], d$)

Input: State s or belief particles \bar{b} , current depth d .

Output: A scalar $\hat{V}_d([s/\bar{b}])$ that is an estimate of $V_d^*([s/\bar{b}])$.

- 1: If $d \geq D$ the max depth, then return 0.
- 2: For $i = 1, \dots, C_a$, run VOO($[s/\bar{b}], q_d, i, d$) with ESTIMATEQ($[s/\bar{b}], a, d$) to obtain $\{q_d([s/\bar{b}], a_i)\}_{i=1}^{C_a}$
- 3: Return the value function:

$$\hat{V}_d([s/\bar{b}]) = \max_{i=1, \dots, C_a} \{q_d([s/\bar{b}], a_i)\}$$

recursive calculation of ESTIMATEV for each of the next-step states since there is no observation uncertainty. On the other hand, VOWSS returns the weighted average of the Q -functions, where all the sampled states s'_i are inserted into each next-step belief particle set \bar{b}_{ao_j} with the new weights $w'_i = w_i \cdot \mathcal{Z}(o_j|a, s'_i)$. Intuitively, these updated weights are the adjusted probability of hypothetically sampling observation o_j from state s'_i . Like sparse sampling and POWSS, both VOSS and VOWSS are not very computationally efficient as they both fully expand out the tree. Thus, they serve the purpose of being theoretically optimal algorithms and are only practically applicable to toy problems.

It is worth noting that with our recursive formulation, Voronoi Optimistic Optimization Tree (VOOT) defined in Kim et al. (2020) can be recast as a Q -function estimation algorithm that simply returns the one sample Q -function estimate. Particularly, this means that ESTIMATEQ for VOOT would look identical to VOSS's ESTIMATEQ function except with C_s set to 1 as VOOT assumes no transition uncertainty, with no action width decay. Consequently, VOOT is notably faster than VOSS and thus practical for deterministic problems, since it only needs to sample the deterministic next step state once. Nevertheless, due to the hierarchical structure of VOOT algorithm definition, the actual VOO algorithm as well as the theoretical guarantees of VOOT should remain identical when recast into this recursive form.

4.2 Convergence Guarantees

Both VOSS and VOWSS value estimates will converge to the optimal value functions for continuous space MDPs and

Algorithm 3 Algorithms for VOSS and VOWSS

Algorithm (VOSS): ESTIMATEQ(s, a, d)

Input: State s , action a , current depth d .

Output: A scalar $\hat{Q}_d(s, a)$ that is an estimate of $Q_d^*(s, a)$.

- 1: For $i = 1, \dots, C_s$, generate $s'_i, r = G(s, a)$.
- 2: Return the Q -value estimate:

$$\hat{Q}_d(s, a) = r + \gamma \frac{1}{C_s} \sum_{i=1}^{C_s} \text{ESTIMATEV}(s'_i, d+1)$$

Algorithm (VOWSS): ESTIMATEQ(\bar{b}, a, d)

Input: Belief particles \bar{b} , action a , current depth d .

Output: A scalar $\hat{Q}_d(\bar{b}, a)$ that is an estimate of $Q_d^*(b, a)$.

- 1: For each particle-weight pair (s_i, w_i) in \bar{b} , generate s'_i, o_i, r_i from $G(s_i, a)$.
- 2: For each observation o_j from previous step, iterate over $i = 1, \dots, C_s$ to insert $(s'_i, w_i \cdot \mathcal{Z}(o_j|a, s'_i))$ to a new belief particle set \bar{b}_{ao_j} .
- 3: Return the Q -value estimate:

$$\hat{Q}_d(\bar{b}, a) = \frac{\sum_{i=1}^{C_s} w_i (r_i + \gamma \cdot \text{ESTIMATEV}(\bar{b}_{ao_i}, d+1))}{\sum_{i=1}^{C_s} w_i}$$

POMDPs, respectively. Combining VOO that globally optimizes over the entire action space and sparse sampling and POWSS that estimate value functions with arbitrary precision, we obtain the global convergence of our value function estimates to the optimal value function. To our knowledge, VOWSS is the first continuous space POMDP algorithm to have global convergence guarantees without relying on any discretization schemes for any of the spaces. In the subsequent sections, we prove that VOSS and VOWSS policies can be made to perform arbitrarily close to the optimal policies by increasing both the state and action widths.

The convergence proofs of our algorithms rely on the proofs for the ancestor algorithms: sparse sampling, POWSS and VOO. Since the proof of VOSS requires the union of all the regularity conditions for sparse sampling and VOO, and the proof of VOWSS the conditions for POWSS and VOO, which mostly deal with local smoothness of rewards and observation density requirements, we will not repeat the exact conditions here. Particularly, one of the conditions require that the reward function R be bounded and measurable, which we denote as $\|R\|_\infty \leq R_{\max}$, and consequently the value is bounded by $V_{\max} \equiv R_{\max}/(1 - \gamma)$ for $\gamma < 1$.

Theorem 1 (VOSS Inequality). Suppose we choose the action sampling width C_a and state sampling width C_s such that under the union of regularity conditions specified by Kearns, Mansour, and Ng (2002) and Kim et al. (2020), the intermediate sparse sampling bounds and VOO bounds in Lemma 1 are satisfied at every depth of the tree. Then, the following bounds for the VOSS estimator $\hat{V}_{\text{VOSS}, d}(s)$ hold for all $d \in [0, D-1]$ in expectation:

$$|V_d^*(s) - \hat{V}_{\text{VOSS}, d}(s)| \leq \eta + \alpha \quad (6)$$

We show a quick outline of the proof of Theorem 1. In order to prove Theorem 1, we first need to prove the intermediate concentration and regret bounds.

Lemma 1 (VOSS Intermediate Inequality). *Suppose with our notation, the sparse sampling estimators at all depths d are within ϵ of their mean values with probability $1 - p$, and the VOO estimators at all depths d have regret bounds of $\eta(d)$. The following inequalities hold for all $d \in [0, D - 1]$ in expectation:*

$$|V_d^*(s) - \hat{V}_d^{C_a}(s)| \leq \eta(d) \quad (7)$$

$$|\hat{V}_d^{C_a}(s) - \hat{V}_{\text{VOSS},d}(s)| \leq \alpha_d \quad (8)$$

In Lemma 1, we aim to bound the inequality in Eq. (1) by applying triangle inequality to the two split terms: the VOO-like regret bound with bound $\eta(d)$ and the sparse sampling-like concentration bound with bound α_d . The exact definitions of these intermediate bound terms are defined and explained further in Appendix A. We define each value function used in Lemma 1 as the following:

$$\begin{aligned} V_d^*(s) &\equiv \max_{a \in \mathcal{A}} \{R(s, a) + \gamma \mathbb{E}[V_{d+1}^*(s')]\} \\ \hat{V}_d^{C_a}(s) &\equiv \max_{a \in \text{VOO}(\mathcal{A})} \{R(s, a) + \gamma \mathbb{E}[\hat{V}_{d+1}^{C_a}(s')]\} \\ \hat{V}_{\text{VOSS},d}(s) &\equiv \max_{a \in \text{VOO}(\mathcal{A})} R(s, a) + \gamma \frac{1}{C_s} \sum_{i=1}^{C_s} \hat{V}_{\text{VOSS},d+1}(s'_i) \end{aligned} \quad (9)$$

Here, $V_d^*(s)$ is the optimal value function as per the conventional definition, and $\hat{V}_{\text{VOSS},d}(s)$ is the VOSS estimator for the optimal value function. In addition, we introduce the theoretical intermediate term $\hat{V}_d^{C_a}(s)$ that bridges the gap between the regret bound and the concentration bound by only performing the VOO step and not the sparse sampling step. Using this intermediate term, we can further subdivide the intermediate inequalities to obtain the appropriate regret and concentration bounds using results from Kim et al. (2020) and Kearns, Mansour, and Ng (2002), respectively. By proving Lemma 1, we can then prove Theorem 1.

Consequently, VOWSS inequality can be defined and proven in a similar way as Theorem 1. VOWSS inequality proof on the other hand will require a little more detail as the calculation is done over the belief space rather than the state space. Full proofs of the lemma and the theorem for both VOSS and VOWSS are given in Appendix A.

Theorem 2 (VOWSS Inequality). *Suppose we choose the action sampling width C_a and state sampling width C_s such that under the union of regularity conditions specified by Lim, Tomlin, and Sunberg (2020) and Kim et al. (2020), the intermediate POWSS bounds and VOO bounds in Lemma 2 are satisfied at every depth of the tree. Then, the following bounds for the VOWSS estimator $\hat{V}_{\text{VOWSS},d}(\bar{b})$ hold for all $d \in [0, D - 1]$ in expectation:*

$$|V_d^*(b) - \hat{V}_{\text{VOWSS},d}(\bar{b})| \leq \eta' + \alpha' \quad (10)$$

Lemma 2 (VOWSS Intermediate Inequality). *Suppose with our notation, the POWSS estimators at all depths d are*

Algorithm 4 Voronoi Progressive Widening

```

1: procedure ACTIONSELECT( $h$ ):
2:   if  $|C(h)| = 0$  then
3:      $a \leftarrow \text{Unif}(\mathcal{A})$ 
4:      $C(h) \leftarrow C(h) \cup \{a\}$ 
5:   else if  $|C(h)| \leq k_a N(h)^{\alpha_0}$  then
6:      $u \leftarrow \text{Unif}[0, 1]$ 
7:     if  $u \leq \omega$  then
8:        $a \leftarrow \text{Unif}(\mathcal{A})$ 
9:     else
10:       $a \leftarrow \text{BESTVORONOICELL}(\mathcal{A}, C(h))$ 
11:       $C(h) \leftarrow C(h) \cup \{a\}$ 
12:    else
13:       $a \leftarrow \arg \max_{a \in C(h)} Q(ha) + c \sqrt{\frac{\log N(h)}{N(ha)}}$ 
14:    return  $a$ 

```

within ϵ' of their mean values with probability $1 - p'$, and the VOO estimators at all depths d have regret bounds of $\eta'(d)$. The following inequalities hold for all $d \in [0, D - 1]$ in expectation:

$$|V_d^*(b) - \hat{V}_d^{C_a}(b)| \leq \eta'(d) \quad (11)$$

$$|\hat{V}_d^{C_a}(b) - \hat{V}_{\text{VOWSS},d}(\bar{b})| \leq \alpha'_d \quad (12)$$

5 Voronoi Progressive Widening

We now introduce Voronoi Progressive Widening (VPW) in Algorithm 4, which combines VOO and PW. Here, h is the belief/history node, $C(h)$ the list of children action nodes, N the number of visits, and c, ω the exploration parameters. Essentially, during the PW step, we probabilistically take a VOO action sample instead of a uniform random action sample. In practice, this VOO action sampling is best implemented by using Gaussian rejection sampling centered around the current best action as noted by Kim et al. (2020), and by terminating when either the candidate action sample is close enough to the best action, or enough samples were rejected that forces us to take the closest sample to the best action so far. Both criteria were used in the experiments in Section 6 to ensure that our samples were sampled close to the best action while keeping the sampling iteration low.

VPW only additionally relies on having a collection of Q -value estimates, which are typically calculated and stored for MCTS solvers. While this means that we require the Q -value estimates to be relatively faithful to the actual Q -values and also requires an informative rollout policy that can guide the solver to more optimal actions, this is not a requirement specific to VPW as a typical MCTS solver should aim to have both of these components. Furthermore, since the VOO step does not require a significant additional time, VPW operates in a similar time scale as PW/DPW while being able to efficiently sample action candidates that are closer to the optimal action. The only other requirement of VPW is the distance metric on the action space, but this is often simple to define, and in fact makes VPW a suitable candidate to also tackle hybrid action spaces as seen in Section 6.2.

The VPW technique is versatile in that it can be applied to any MCTS solvers for MDPs and POMDPs without requiring any additional expert or domain knowledge. For instance, one could consider Sparse-UCT-VPW algorithm for continuous space MDPs that uses VPW criterion with the Sparse-UCT algorithm (Bjarnason, Fern, and Tadelpalli 2009) to handle continuous action spaces. For POMDP solvers, we demonstrate the versatility of VPW through modifying POMCPOW into VOMCPOW (Voronoi Optimistic Monte Carlo Planning with Observation Weighting) by simply swapping out action PW with VPW. In theory, this can be done the same way for PFT-DPW to make PFT-VPW instead, but we only show results for VOMCPOW, which already outperforms POMCPOW and BOMCP by a statistically significant margin across all of our experiments.

6 Experiments

The numerical experiments in this section confirm the theoretical results of Section 4.2, as well as showcase the effectiveness of VPW. We demonstrate the performances of our algorithms in three different experiments: Linear-Quadratic-Gaussian (LQG) control, Van Der Pol Tag, and lunar lander problems. When running experiments for POMCPOW, VOMCPOW, and BOMCP, we use the rollout policy heuristic to estimate the value function as well as take the first action to be the rollout policy action at each newly generated belief node. To determine the hyperparameters of the solvers, we used cross-entropy method (CEM) (Mannor, Rubinstein, and Gat 2003) to maximize the mean expected reward of a hyperparameter set when the optimal hyperparameters are not already available from previous experiments. The VOMCPOW and BOMCP hyperparameters were trained by first initializing them with POMCPOW hyperparameters and then using the CEM again including all the additional hyperparameters specific to the solvers. The only hyperparameter that was manually picked is the Gaussian covariance matrix for VOO rejection sampling. The code for the experiments is built on the POMDPs.jl framework (Egorov et al. 2017). The exact hyperparameters used for each experiment are given in Appendix B.

6.1 Linear-Quadratic-Gaussian Control

We first test our algorithms on a simple 2D-action space LQG control system. Here, we define the LQG system to be relatively simple such that we can easily understand and visualize the results while allowing VOWSS to still plan within a reasonable time. We define the dynamics and observation models as following:

$$x_{t+1} = x_t + u_t + v_t \quad v_t \stackrel{i.i.d.}{\sim} N(0, \sigma^2 I) \quad (13)$$

$$y_t = x_t + w_t \quad w_t \stackrel{i.i.d.}{\sim} N(0, \sigma^2 I) \quad (14)$$

The initial state x_0 is distributed as $N([-10, 10], \sigma^2 I)$, and $\sigma = 0.1$ for all x_0, v_t, w_t . We aim to minimize the cost function $J(x_0)$, while planning for two steps ($N = 2$):

$$J(x_0) = \mathbb{E} \left[x_N^T x_N + \sum_{t=0}^{N-1} (x_t^T x_t + u_t^T u_t) \right] \quad (15)$$

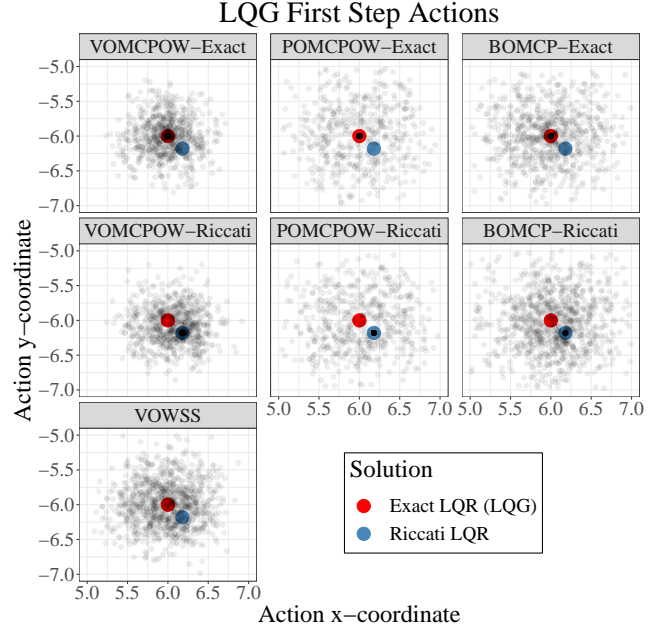


Figure 2: Scatter plots of the first actions chosen by different solvers and rollout policies for the two step LQG problem. The exact LQR solution, which is the same as the LQG solution, is shown as a red dot at $[6.0, -6.0]$, and the Riccati solution is shown as a blue dot at approximately $[6.18, -6.18]$.

The analytical answer can be obtained by solving the LQG backup equation, which is identical to the LQR solution:

$$u_0^* = -K_0 \hat{x}_0 = -0.6 \cdot \hat{x}_0 = [6.0, -6.0] \quad (16)$$

Since the problem is theoretically tractable, we can directly compare the actions each solver chooses to the analytical solution, for VOWSS, POMCPOW, VOMCPOW and BOMCP. For the solvers that require a rollout policy, we test both finite horizon LQR solution (referred to as “exact policy”) and the discrete time algebraic Riccati solution (referred to as “Riccati policy”) (Chow 1975) as the rollout policies on the mean of the belief to see how that affects the performances of each solver. In this problem setup, the fact that we only plan for two steps into the future means that our Riccati policy will not be as close to optimal as the exact policy. As a reference, the Riccati policy solution at all times is given by $u_t^* \approx -0.618 \cdot \hat{x}_t$ for this particular setup, which makes the optimal action for first step be $u_0^* \approx [6.18, -6.18]$.

When choosing hyperparameters through CEM, we use the Riccati policy as the rollout policy. The number of queries for POMCPOW and VOMCPOW are set to 1000 and BOMCP to 100, which correspond to approximately 0.1 seconds of planning time. For VOWSS, the state width is set to 10 and action width to 200. Furthermore, we introduce the action width decay term γ_a such that the number of VOO iterations for a given height of the tree is given as γ_a times the VOO iterations for the previous height, similar to how Kim et al. (2020) define VOOT to solve longer horizon

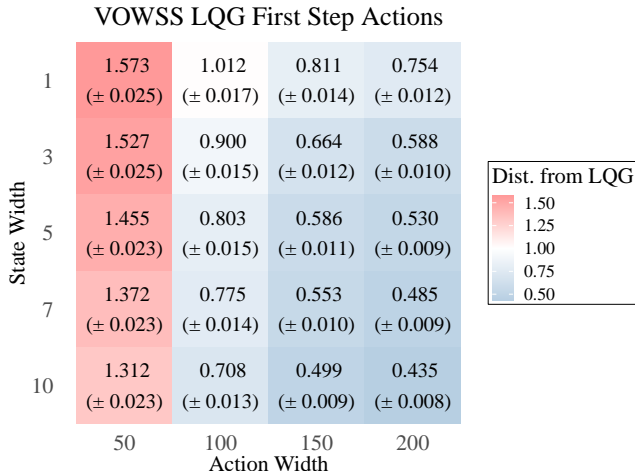


Figure 3: Tabular summary of the first actions chosen by VOWSS, where we show the mean Euclidean distance to the LQG solution, and the corresponding standard error in parentheses.

tasks. The action width decay is manually set to $\gamma_a = 0.4$ after a careful inspection to balance performance and run time, which means that the action width for first step is 200, and the action width for second step is 80. While this results in number of evaluations on the order of 10^6 , we include the performance of VOWSS action selection as a reference.

We first show the scatter plots of how each solver chooses the first step action in Figure 2. Each scatter plot shows the result of 1000 simulations. While POMCPOW and BOMCP suffer from biasing their solution towards the rollout actions, we see that the effect is much less pronounced in VOMCPOW. Especially, when the rollout policy is set to Riccati policy, both POMCPOW and BOMCP heavily resort to picking the Riccati solution as shown by the large point mass corresponding to the Riccati solution in the scatter plots. Even though VOMCPOW still produces a sizable mass of points on and surrounding the Riccati solution, it otherwise picks solutions that are not very far away from the LQG solution. VOMCPOW scatter plots show that the bias and the variance of the optimal action estimates are noticeably smaller than those of POMCPOW and BOMCP. Although VOWSS cannot be directly compared to the other solvers since the number of iterations is not on the same order and it doesn't rely on a rollout policy, the overall shape of the scatter plot looks similar to those of VOMCPOW.

In addition, we study the effects of varying the state and action widths for VOWSS. Figure 3 shows the table of mean Euclidean distance to the LQG solution for different combinations of state and action width, as well as the corresponding standard error in parentheses. Each cell in the table shows the result of 1000 simulations, and the other hyperparameters are left intact. As we increase either the state or action width, the mean distance and the standard error decrease. This indicates that VOWSS solver chooses better actions by increasing the state and action widths, which is expected as larger state widths should increase the accuracy

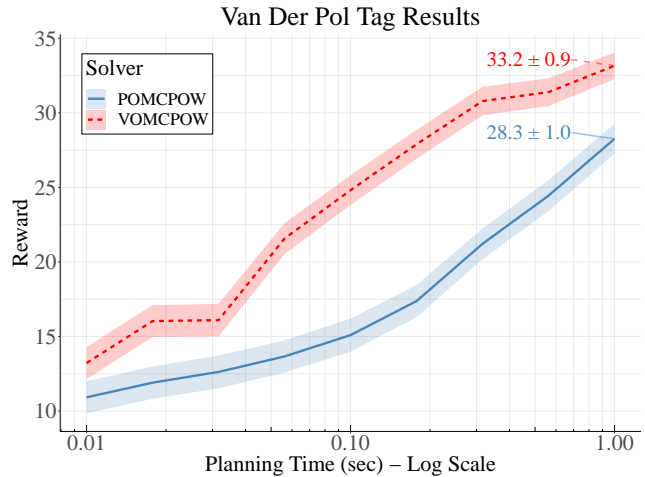


Figure 4: Mean rewards for POMCPOW and VOMCPOW for VDP Tag. Ribbons indicate one standard error.

of value function calculation and larger action widths should improve optimization over the action space.

6.2 Van Der Pol Tag

Next, we test POMCPOW and VOMCPOW on the Van Der Pol Tag (VDP Tag) problem introduced by Sunberg and Kochenderfer (2018), which is their only problem with continuous state, action and observation spaces. In VDP Tag, an agent navigates through 2D box to tag a target with randomized initial state and following a dynamics model defined by the Van Der Pol differential equation. The agent moves at a fixed speed, but can choose the direction of travel and decide to make an accurate observation of where the target is at a higher cost than making the default noisy observation. While the target can freely move within the 2D box, the agent is blocked when it comes into contact with one of the cardinal barriers.

We show the mean reward for 1000 simulations for each solver and each planning time plotted in log scale of seconds in Figure 4. We observe that VOMCPOW outperforms POMCPOW at every planning time by a statistically significant margin. It is also worth noting that VOMCPOW takes almost an order of magnitude less planning time to reach the mean reward of 25 compared to POMCPOW. While VDP Tag is a continuous space POMDP, the rewards are still discrete in both state and action spaces, which suggests that even with discrete jumps in the reward function, VPW can still optimize to find better actions. In addition, while it is possible to adapt BOMCP to solve VDP Tag, it requires nontrivial modifications to the action space due to the action space being hybrid ($\mathcal{A} = [0, 2\pi] \times \{0, 1\}$) and the angle space being a modular space. This further illustrates the ease of implementing VPW since we only need to supply VPW with a distance metric on the action space, which makes VPW suitable for hybrid action spaces as well.

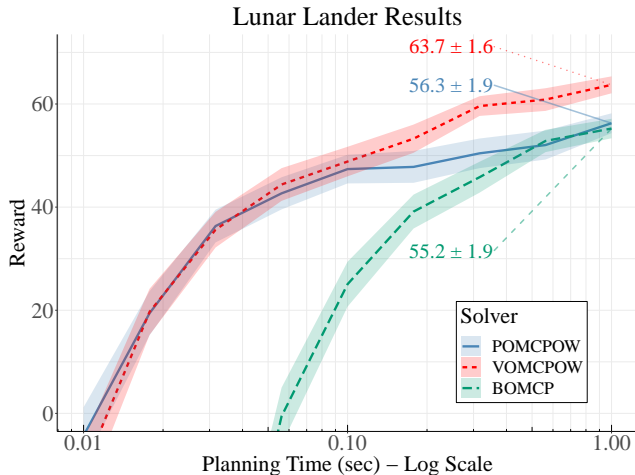


Figure 5: Mean rewards for POMCPOW, VOMCPOW and BOMCP for the modified lunar lander problem. Ribbons indicate one standard error.

6.3 Lunar Lander

Lastly, we test POMCPOW, VOMCPOW and BOMCP on the modified lunar lander problem proposed by Mern et al. (2021b), where the main objective is to guide a vehicle to land in a target zone safely. In this version of lunar lander, the vehicle state is defined as $(x, y, \theta, \dot{x}, \dot{y}, \omega)$, and we only obtain noisy observations of the angular rate, horizontal speed, and above-ground level. The action space is defined by the tuple (T, F_x, δ) where T is the main vertical thrust, F_x the corrective horizontal thrust, and δ the offset. The default rollout policy is proportional control based on the observation.

Once again, we show the mean reward for 1000 simulations for each solver and each planning time plotted in log scale of seconds in Figure 5. VOMCPOW outperforms both POMCPOW and BOMCP by a statistically significant margin once the planning time exceeds 0.1 seconds. Below 0.1 seconds, the performances of POMCPOW and VOMCPOW are very similar due to the problem having a long planning horizon, in which the effects of VPW will not be as apparent since new actions will not be sampled very often from the VOO component of VPW.

We note that the performance of POMCPOW here is seemingly vastly different from the analyses done in Mern et al. (2021b), which might be due to a several factors. The lander problem has a high variance in the returns, since failure to land results in a steep penalty of -1000. This failure mode does not happen very often even within 1000 iterations, so the number of failures significantly impacts the mean rewards. Furthermore, we are comparing the algorithms based on planning time rather than number of queries. POMCPOW queries much faster than BOMCP, and average planning time may not sufficiently capture the relationship between total planning time and number of queries for a progressively built tree.

7 Conclusion

In this paper, we have introduced Voronoi Progressive Widening (VPW), a versatile technique to effectively handle continuous or hybrid action spaces in MDPs and POMDPs. Consequently, we proposed three VPW-based tree search algorithms with convergence guarantees or efficiency, justifying the theoretical soundness, versatility and practicality of VPW for many continuous or hybrid action space MDPs and POMDPs.

This study has yielded a several key insights, which suggest some promising future directions to explore. While each of the VPW-based algorithms either enjoy theoretical guarantees or computational efficiency, the gap between theoretical soundness and practicality still remains. In particular, the state and action selection heuristics as it is utilized in POMCPOW still need to be integrated into the theoretical algorithms like POWSS to bridge the gap between theory and practice. On the other hand, we believe that the VPW technique itself should also have some theoretical guarantees similar to the DPW technique (Couëtoux et al. 2011).

It could be worthwhile to explore whether VPW would be more effective for belief state MDP planners like PFT-DPW or state trajectory based POMDP planners like POMCPOW for solving continuous or hybrid action space POMDPs. Additionally, since the convergence guarantees of VOO hold as long as the reward function is locally smooth around at least one global optimum (Kim et al. 2020), more extensive study could be done for effectiveness of VPW on MDPs and POMDPs with discrete reward structures. Similar to how the Rényi divergence requirement for POWSS (Lim, Tomlin, and Sunberg 2020) could be a difficulty indicator for likelihood-weighted sparse tree solvers, the proof techniques utilized for VOO and DPW could offer insights on what continuous or hybrid action space problems are harder to solve than others.

Acknowledgements

This material is based upon work supported by a DARPA Assured Autonomy Grant, the SRC CONIX program, NSF CPS Frontiers, the ONR Embedded Humans MURI, and the National Science Foundation Graduate Research Fellowship Program under Grant No. DGE 1752814. Any opinions, findings, and conclusions or recommendations expressed in this material are those of the authors and do not necessarily reflect the views of any aforementioned organizations. The authors also thank John Mern for sharing the source code for BOMCP and the lunar lander environment, and providing valuable insights as well as technical support for running and verifying these scripts.

References

- Ayer, T.; Alagoz, O.; and Stout, N. K. 2012. A POMDP approach to personalize mammography screening decisions. *Operations Research* 60(5): 1019–1034.
- Bai, H.; Cai, S.; Ye, N.; Hsu, D.; and Lee, W. S. 2015. Intention-Aware Online POMDP Planning for Autonomous Driving in a Crowd. In *IEEE International Conference*

on Robotics and Automation, 454–460. Seattle, WA, USA: IEEE.

Bertsekas, D. 2005. *Dynamic Programming and Optimal Control*. Massachusetts: Athena Scientific.

Bjarnason, R.; Fern, A.; and Tadepalli, P. 2009. Lower bounding Klondike solitaire with Monte-Carlo planning. In *International Conference on Automated Planning and Scheduling*. Thessaloniki, Greece: AAAI Press.

Browne, C. B.; Powley, E.; Whitehouse, D.; Lucas, S. M.; Cowling, P. I.; Rohlfsagen, P.; Tavener, S.; Perez, D.; Samothrakis, S.; and Colton, S. 2012. A Survey of Monte Carlo Tree Search Methods. *IEEE Transactions on Computational Intelligence and AI in Games* 4(1): 1–43.

Chow, G. 1975. *Analysis and Control of Dynamic Economic Systems*. New York: John Wiley & Sons.

Couëtoux, A.; Hoock, J.-B.; Sokolovska, N.; Teytaud, O.; and Bonnard, N. 2011. Continuous Upper Confidence Trees. In *Learning and Intelligent Optimization*. Rome, Italy: Springer.

Egorov, M.; Sunberg, Z. N.; Balaban, E.; Wheeler, T. A.; Gupta, J. K.; and Kochenderfer, M. J. 2017. POMDPs.jl: A Framework for Sequential Decision Making under Uncertainty. *Journal of Machine Learning Research* 18(26): 1–5.

Holland, J. E.; Kochenderfer, M. J.; and Olson, W. A. 2013. Optimizing the Next Generation Collision Avoidance System for Safe, Suitable, and Acceptable Operational Performance. *Air Traffic Control Quarterly* 21(3): 275–297.

Kaelbling, L. P.; Littman, M. L.; and Cassandra, A. R. 1998. Planning and acting in partially observable stochastic domains. *Artificial Intelligence* 101(1): 99 – 134.

Kearns, M.; Mansour, Y.; and Ng, A. Y. 2002. A Sparse Sampling Algorithm for Near-Optimal Planning in Large Markov Decision Processes. *Machine Learning* 49(2): 193–208.

Kim, B.; Lee, K.; Lim, S.; Kaelbling, L.; and Lozano-Perez, T. 2020. Monte Carlo Tree Search in Continuous Spaces Using Voronoi Optimistic Optimization with Regret Bounds. In *AAAI Conference on Artificial Intelligence*, volume 34, 9916–9924. AAAI Press.

Kochenderfer, M. J. 2015. *Decision Making Under Uncertainty: Theory and Application*. Massachusetts: MIT Press.

Kurniawati, H.; and Yadav, V. 2016. An online POMDP solver for uncertainty planning in dynamic environment. In *Robotics Research*, 611–629. Springer.

Lee, J.; Jeon, W.; Kim, G.-H.; and Kim, K.-E. 2020. Monte-Carlo Tree Search in Continuous Action Spaces with Value Gradients. In *AAAI Conference on Artificial Intelligence*, volume 34, 4561–4568. AAAI Press.

Lim, M. H.; Tomlin, C.; and Sunberg, Z. N. 2020. Sparse Tree Search Optimality Guarantees in POMDPs with Continuous Observation Spaces. In *International Joint Conference on Artificial Intelligence, IJCAI-20*, 4135–4142. International Joint Conferences on Artificial Intelligence, Inc.

Mannor, S.; Rubinstein, R.; and Gat, Y. 2003. The Cross Entropy Method for Fast Policy Search. In *International Conference on Machine Learning*, 512–519. AAAI Press.

Mansley, C.; Weinstein, A.; and Littman, M. L. 2011. Sample-Based Planning for Continuous Action Markov Decision Processes. In *International Conference on Automated Planning and Scheduling*, 335–338. AAAI Press.

Mao, W.; Zhang, K.; Xie, Q.; and Başar, T. 2020. POLY-HOOT: Monte-Carlo Planning in Continuous Space MDPs with Non-Asymptotic Analysis. In *Advances in Neural Information Processing Systems*, volume 33. Curran Associates, Inc.

Mern, J.; Yıldız, A.; Bush, L.; Mukerji, T.; and Kochenderfer, M. J. 2021a. Improved POMDP Tree Search Planning with Prioritized Action Branching. In *AAAI Conference on Artificial Intelligence*. AAAI Press.

Mern, J.; Yıldız, A.; Sunberg, Z.; Mukerji, T.; and Kochenderfer, M. J. 2021b. Bayesian optimized Monte Carlo planning. In *AAAI Conference on Artificial Intelligence*. AAAI Press.

Morere, P.; Marchant, R.; and Ramos, F. 2016. Bayesian Optimisation for solving Continuous State-Action-Observation POMDPs. In *Advances in Neural Information Processing Systems*, volume 30. Curran Associates, Inc.

Papadimitriou, C. H.; and Tsitsiklis, J. N. 1987. The Complexity of Markov Decision Processes. *Mathematics of Operations Research* 12(3): 441–450.

Seiler, K. M.; Kurniawati, H.; and Singh, S. P. N. 2015. An online and approximate solver for POMDPs with continuous action space. In *IEEE International Conference on Robotics and Automation*, 2290–2297. IEEE.

Silver, D.; and Veness, J. 2010. Monte-Carlo Planning in Large POMDPs. In *Advances in Neural Information Processing Systems*, 2164–2172. Curran Associates, Inc.

Sunberg, Z.; and Kochenderfer, M. J. 2018. Online Algorithms for POMDPs with Continuous State, Action, and Observation Spaces. In *International Conference on Automated Planning and Scheduling*. Delft, Netherlands: AAAI Press.

Sunberg, Z. N.; Ho, C. J.; and Kochenderfer, M. J. 2017. The Value of Inferring the Internal State of Traffic Participants for Autonomous Freeway Driving. In *American Control Conference*, 3004–3010. Seattle, WA, USA: IEEE.

Weinstein, A.; and Littman, M. L. 2012. Bandit-Based Planning and Learning in Continuous-Action Markov Decision Processes. In *International Conference on Automated Planning and Scheduling*, 306–314. AAAI Press.

Ye, N.; Soman, A.; Hsu, D.; and Lee, W. S. 2017. DESPOT: Online POMDP Planning with Regularization. *Journal of Artificial Intelligence Research* 58: 231–266.

Young, S.; Gašić, M.; Thomson, B.; and Williams, J. D. 2013. POMDP-based statistical spoken dialog systems: A review. *IEEE* 101(5): 1160–1179.

Appendix

Appendix for “Voronoi Progressive Widening: Efficient Online Solvers for Continuous Space MDPs and POMDPs with Provably Optimal Components”

Table of Contents

A Mathematical Proofs	1
A.1 Voronoi Optimistic Sparse Sampling (VOSS)	1
A.2 Voronoi Optimistic Weighted Sparse Sampling (VOWSS)	4
B Experiment Hyperparameters	9

A Mathematical Proofs

A.1 Voronoi Optimistic Sparse Sampling (VOSS)

Theorem 1 (VOSS Inequality). *Suppose we choose the action sampling width C_a and state sampling width C_s such that under the union of regularity conditions specified by Kearns, Mansour, and Ng (2002) and Kim et al. (2020), the intermediate sparse sampling bounds and VOO bounds in Lemma 1 are satisfied at every depth of the tree. Then, the following bounds for the VOSS estimator $\hat{V}_{\text{VOSS},d}(s)$ hold for all $d \in [0, D-1]$ in expectation:*

$$\left| V_d^*(s) - \hat{V}_{\text{VOSS},d}(s) \right| \leq \eta + \alpha \quad (1)$$

In order to prove Theorem 1, we first prove an intermediate lemma which will allow us to obtain the bound through triangle inequality. We introduce and prove the following lemma first. All of the following calculations are done in expectation.

Lemma 1 (VOSS Intermediate Inequality). *Suppose with our notation, the sparse sampling estimators at all depths d are within ϵ of their mean values with probability $1 - p$, and the VOO estimators at all depths d have regret bounds of $\eta(d)$. The following inequalities hold for all $d \in [0, D-1]$ in expectation:*

$$\left| V_d^*(s) - \hat{V}_d^{C_a}(s) \right| \leq \eta(d) \quad (2)$$

$$\left| \hat{V}_d^{C_a}(s) - \hat{V}_{\text{VOSS},d}(s) \right| \leq \alpha_d \quad (3)$$

\mathcal{R}_{C_a} is the regret of VOO after taking C_a samples, and $\eta(d)$ and α_d are defined and upper bounded as:

$$\alpha_d \equiv \gamma(\alpha_{d+1} + \epsilon + 2p \cdot V_{\max}), \quad \alpha_{D-1} = \epsilon + 2p \cdot V_{\max} \quad (4)$$

$$\eta(d) \equiv \gamma \cdot \eta(d+1) + \mathcal{R}_{C_a}, \quad \eta(D) = 0 \quad (5)$$

$$\eta \equiv \max_{d=0, \dots, D-1} \eta(d), \quad \alpha \equiv \max_{d=0, \dots, D-1} \alpha_d \quad (6)$$

Proof. This proceeds by induction by assuming that the equality holds for all depths from $d+1$ to $D-1$, and then proving it is also true for depth d (induction hypothesis is omitted as they trivially hold as per the definitions of VOOT and sparse sampling). We divide the main inequality into VOO bound and sparse sampling bound (SS bound) by introducing an intermediate term $\hat{V}_d^{C_a}(s)$:

$$\left| V_d^*(s) - \hat{V}_{\text{VOSS},d}(s) \right| \leq \underbrace{\left| V_d^*(s) - \hat{V}_d^{C_a}(s) \right|}_{\text{VOO bound}} + \underbrace{\left| \hat{V}_d^{C_a}(s) - \hat{V}_{\text{VOSS},d}(s) \right|}_{\text{SS bound}} \quad (7)$$

Essentially, we now have two main layers of inequality, caused by uncertainty in state transition and the stochastic nature of VOO action selection. We will first analyze the VOO bound, then the SS bound.

(i) VOO Bound The VOO bound can be further decomposed into the following terms as Kim et al. (2020) do in their work:

$$\left| V_d^*(s) - \hat{V}_d^{C_a}(s) \right| \leq \underbrace{\left| V_d^*(s) - \hat{V}_d(s) \right|}_{\text{VOO Recursive bound}} + \underbrace{\left| \hat{V}_d(s) - \hat{V}_d^{C_a}(s) \right|}_{\text{VOO Regret bound}} \quad (8)$$

Here, the intermediate random variables are defined in the following manner:

$$V_d^*(s) \equiv \max_{a \in \mathcal{A}} Q_d^*(s, a) = \max_{a \in \mathcal{A}} \left\{ R(s, a) + \gamma \mathbb{E}_{s' \sim T(s, a)} [V_{d+1}^*(s')] \right\} \quad (9)$$

$$\hat{V}_d(s) \equiv \max_{a \in \mathcal{A}} \hat{Q}_d(s, a) = \max_{a \in \mathcal{A}} \left\{ R(s, a) + \gamma \mathbb{E}_{s' \sim T(s, a)} [\hat{V}_{d+1}^{C_a}(s')] \right\} \quad (10)$$

$$\hat{V}_d^{C_a}(s) \equiv \max_{a \in VOO(\mathcal{A}, C_a)} \hat{Q}_d(s, a) = \max_{a \in VOO(\mathcal{A}, C_a)} \left\{ R(s, a) + \gamma \mathbb{E}_{s' \sim T(s, a)} [\hat{V}_{d+1}^{C_a}(s')] \right\} \quad (11)$$

As a notation, $a \in VOO(\mathcal{A}, C_a)$ indicates that the actions a are chosen sequentially through the VOO algorithm over the action space \mathcal{A} for C_a iterations of VOO. Here, we compare the two quantities with a reference action $a^* = \arg \max Q_d^*(s, a)$, which results in a looser bound but allows us to directly compare the quantities inside the max operations. We closely follow the calculations from the proof of Lemma 5 in Kim et al. (2020):

$$\underbrace{|V_d^*(s) - \hat{V}_d(s)|}_{\text{VOO Recursive bound}} = \left| \max_{a \in \mathcal{A}} \left\{ R(s, a) + \gamma \mathbb{E}_{s' \sim T(s, a)} [V_{d+1}^*(s')] \right\} - \max_{a \in \mathcal{A}} \left\{ R(s, a) + \gamma \mathbb{E}_{s' \sim T(s, a)} [\hat{V}_{d+1}^{C_a}(s')] \right\} \right| \quad (12)$$

$$\leq \left| R(s, a^*) + \gamma \mathbb{E}_{s' \sim T(s, a^*)} [V_{d+1}^*(s')] - R(s, a^*) - \gamma \mathbb{E}_{s' \sim T(s, a^*)} [\hat{V}_{d+1}^{C_a}(s')] \right| \quad (a^* = \arg \max Q_d^*(s, a))$$

$$\leq \gamma \mathbb{E}_{s' \sim T(s, a^*)} |V_{d+1}^*(s') - \hat{V}_{d+1}^{C_a}(s')| \quad (13)$$

$$\leq \gamma \cdot \eta(d+1) \quad (14)$$

$$\underbrace{|\hat{V}_d(s) - \hat{V}_d^{C_a}(s)|}_{\text{VOO Regret bound}} \leq \mathcal{R}_{C_a} \quad (15)$$

In the VOO Regret bound, the difference cannot be less than zero since the global maximum is at least as big as the VOO maximum, so the absolute value disappears and we get the regret of VOO. Thus, with our choice of C_a that is designed to satisfy the recurrence relation, we obtain the bound:

$$|V_d^*(s) - \hat{V}_d^{C_a}(s)| \leq \underbrace{|V_d^*(s) - \hat{V}_d(s)|}_{\text{VOO Recursive bound}} + \underbrace{|\hat{V}_d(s) - \hat{V}_d^{C_a}(s)|}_{\text{VOO Regret bound}} \quad (16)$$

$$\leq \gamma \cdot \eta(d+1) + \mathcal{R}_{C_a} = \eta(d) \quad (17)$$

(ii) Sparse Sampling Bound The SS bound can also be further decomposed into the following terms:

$$|\hat{V}_d^{C_a}(s) - \hat{V}_{\text{VOSS}, d}(s)| \leq \underbrace{|\hat{V}_d^{C_a}(s) - \tilde{V}_{\text{VOSS}, d}(s)|}_{\text{SS Concentration bound}} + \underbrace{|\tilde{V}_{\text{VOSS}, d}(s) - \hat{V}_{\text{VOSS}, d}(s)|}_{\text{SS Recursive bound}} \quad (18)$$

Here, the extra intermediate random variable and the VOSS estimator are defined in the following manner:

$$\tilde{V}_{\text{VOSS}, d}(s) \equiv \max_{a \in VOO(\mathcal{A}, C_a)} \tilde{Q}_{\text{VOSS}, d}(s, a) = \max_{a \in VOO(\mathcal{A}, C_a)} \left\{ R(s, a) + \gamma \frac{1}{C_s} \sum_{i=1}^{C_s} \hat{V}_{d+1}^{C_a}(s'_i) \right\} \quad (19)$$

$$\hat{V}_{\text{VOSS}, d}(s) \equiv \max_{a \in VOO(\mathcal{A}, C_a)} \hat{Q}_{\text{VOSS}, d}(s, a) = \max_{a \in VOO(\mathcal{A}, C_a)} \left\{ R(s, a) + \gamma \frac{1}{C_s} \sum_{i=1}^{C_s} \hat{V}_{\text{VOSS}, d+1}(s'_i) \right\} \quad (20)$$

We now apply the sparse sampling bound as well as the recursive bound in order to bound the SS bound components. In our case, since our sparse sampling term $\hat{V}_{\text{VOSS}, d}(s)$ is merely swapping out the expectation of $\hat{V}_{d+1}^{C_a}$ with a sample average under the appropriate sampling density, this turns out to be simply the Chernoff bound. We transform the sparse sampling concentration bound to an expected value bound by using the fact that the difference of V functions/estimators is bounded above by $2V_{\max}$, setting the concentration bound to be ϵ as per the Lemma statement and assigning the worse-case result with probability p . Once

again, we compare the two quantities by picking a reference action to directly compare the quantities inside the max operations:

$$\underbrace{\left| \hat{V}_d^{C_a}(s) - \tilde{V}_{\text{VOSS},d}(s) \right|}_{\text{SS Concentration bound}} \leq \left| \max_{a \in \text{VOO}(\mathcal{A}, C_a)} \{R(s, a) + \gamma \mathbb{E}_{s' \sim T(s, a)} [\hat{V}_{d+1}^{C_a}(s')]\} - \max_{a \in \text{VOO}(\mathcal{A}, C_a)} \{R(s, a) + \gamma \frac{1}{C_s} \sum_{i=1}^{C_s} \hat{V}_{d+1}^{C_a}(s'_i)\} \right| \quad (21)$$

$$\begin{aligned} &\leq \gamma \left| \mathbb{E}_{s' \sim T(s, a^*)} [\hat{V}_{d+1}^{C_a}(s')] - \frac{1}{C_s} \sum_{i=1}^{C_s} \hat{V}_{d+1}^{C_a}(s'_i) \right| \quad (a^* = \arg \max_{\text{VOO}} \hat{Q}_d(s, a)) \\ &\leq \gamma \cdot ((1-p)\epsilon + 2p \cdot V_{\max}) \leq \gamma \cdot (\epsilon + 2p \cdot V_{\max}) \end{aligned} \quad (22)$$

For the SS Recursive bound, we simply apply the inductive hypothesis:

$$\underbrace{\left| \tilde{V}_{\text{VOSS},d}(s) - \hat{V}_{\text{VOSS},d}(s) \right|}_{\text{SS Recursive bound}} \leq \left| \max_{a \in \text{VOO}(\mathcal{A}, C_a)} \{R(s, a) + \gamma \frac{1}{C_s} \sum_{i=1}^{C_s} \hat{V}_{d+1}^{C_a}(s'_i)\} \right. \quad (23)$$

$$\left. - \max_{a \in \text{VOO}(\mathcal{A}, C_a)} \{R(s, a) + \gamma \frac{1}{C_s} \sum_{i=1}^{C_s} \hat{V}_{\text{VOSS},d+1}(s'_i)\} \right| \quad (24)$$

$$\begin{aligned} &\leq \gamma \frac{1}{C_s} \sum_{i=1}^{C_s} \left| \hat{V}_{d+1}^{C_a}(s'_i) - \hat{V}_{\text{VOSS},d+1}(s'_i) \right| \Big|_{s'_i \sim T(s, \tilde{a})} \quad (\tilde{a} = \arg \max_{\text{VOO}} \tilde{Q}_{\text{VOSS},d}(s, a)) \\ &\leq \gamma \cdot \alpha_{d+1} \end{aligned} \quad (25)$$

Putting the sparse sampling components together by applying the recursive definition of α_d , we obtain the recurring concentration inequality by induction:

$$\left| \hat{V}_d^{C_a}(s) - \hat{V}_{\text{VOSS},d}(s) \right| \leq \underbrace{\left| \hat{V}_d^{C_a}(s) - \tilde{V}_{\text{VOSS},d}(s) \right|}_{\text{SS Concentration bound}} + \underbrace{\left| \tilde{V}_{\text{VOSS},d}(s) - \hat{V}_{\text{VOSS},d}(s) \right|}_{\text{SS Recursive bound}} \quad (26)$$

$$\leq \gamma \cdot (\epsilon + 2p \cdot V_{\max}) + \gamma \cdot \alpha_{d+1} = \alpha_d \blacksquare \quad (27)$$

Proof for Theorem 1. Finally, we prove the main theorem by combining the two terms:

$$\left| V_d^*(s) - \hat{V}_{\text{VOSS},d}(s) \right| \leq \underbrace{\left| V_d^*(s) - \hat{V}_d^{C_a}(s) \right|}_{\text{VOO bound}} + \underbrace{\left| \hat{V}_d^{C_a}(s) - \hat{V}_{\text{VOSS},d}(s) \right|}_{\text{SS bound}} \leq \eta(d) + \alpha_d \leq \eta + \alpha \blacksquare \quad (28)$$

A.2 Voronoi Optimistic Weighted Sparse Sampling (VOWSS)

Theorem 2 (VOWSS Inequality). *Suppose we choose the action sampling width C_a and state sampling width C_s such that under the union of regularity conditions specified by Lim, Tomlin, and Sunberg (2020) and Kim et al. (2020), the intermediate POWSS bounds and VOO bounds in Lemma 2 are satisfied at every depth of the tree. Then, the following bounds for the VOWSS estimator $\hat{V}_{\text{VOWSS},d}(\bar{b})$ hold for all $d \in [0, D - 1]$ in expectation:*

$$\left| V_d^*(b) - \hat{V}_{\text{VOWSS},d}(\bar{b}) \right| \leq \eta' + \alpha' \quad (29)$$

Similar to proving Theorem 1, to prove Theorem 2, we first prove an intermediate lemma which will allow us to obtain the bound through triangle inequality. We introduce and prove the following lemma first. All of the following calculations are done in expectation. We also denote \bar{b} for a particle representation of belief b that POWSS and VOWSS take as an argument.

Lemma 2 (VOWSS Intermediate Inequality). *Suppose with our notation, the POWSS estimators at all depths d are within ϵ' of their mean values with probability $1 - p'$, and the VOO estimators at all depths d have regret bounds of $\eta'(d)$. The following inequalities hold for all $d \in [0, D - 1]$ in expectation:*

$$\left| V_d^*(b) - \hat{V}_d^{C_a}(b) \right| \leq \eta'(d) \quad (30)$$

$$\left| \hat{V}_d^{C_a}(b) - \hat{V}_{\text{VOWSS},d}(\bar{b}) \right| \leq \alpha'_d \quad (31)$$

\mathcal{R}_{C_a} is the regret of VOO after taking C_a samples, and $\eta'(d)$ and α'_d are defined and upper bounded as:

$$\alpha'_d \equiv (1 + \gamma)(\epsilon' + 2p' \cdot V_{\max}) + \gamma(\alpha'_{d+1} + 2p' \cdot V_{\max}), \quad \alpha'_{D-1} = \epsilon' + 2p' \cdot V_{\max} \quad (32)$$

$$\eta'(d) \equiv \gamma \cdot \eta'(d+1) + \mathcal{R}_{C_a}, \quad \eta'(D) = 0 \quad (33)$$

$$\eta' \equiv \max_{d=0, \dots, D-1} \eta'(d), \quad \alpha' \equiv \max_{d=0, \dots, D-1} \alpha'_d \quad (34)$$

Proof. Once again, this proceeds by induction by assuming that the equality holds for all depths from $d + 1$ to $D - 1$, and then proving it is also true for depth d (induction hypothesis is omitted as they trivially hold as per the definitions of VOOT and POWSS). We divide the main inequality into VOO bound and POWSS bound by introducing an intermediate term $\hat{V}_d^{C_a}(b)$:

$$\left| V_d^*(b) - \hat{V}_{\text{VOWSS},d}(\bar{b}) \right| \leq \underbrace{\left| V_d^*(b) - \hat{V}_d^{C_a}(b) \right|}_{\text{VOO bound}} + \underbrace{\left| \hat{V}_d^{C_a}(b) - \hat{V}_{\text{VOWSS},d}(\bar{b}) \right|}_{\text{POWSS bound}} \quad (35)$$

We have two main layers of inequality, caused by uncertainties in state transition and observation, and the stochastic nature of VOO action selection. We will first analyze the VOO bound, then the POWSS bound.

(i) VOO Bound The VOO bound can once again be further decomposed into the following terms as Kim et al. (2020) do in their work:

$$\left| V_d^*(b) - \hat{V}_d^{C_a}(b) \right| \leq \underbrace{\left| V_d^*(b) - \hat{V}_d(b) \right|}_{\text{VOO Recursive bound}} + \underbrace{\left| \hat{V}_d(b) - \hat{V}_d^{C_a}(b) \right|}_{\text{VOO Regret bound}} \quad (36)$$

This step is very close to our previous procedure in VOSS. Here, the intermediate random variables are defined in the following manner:

$$V_d^*(b) \equiv \max_{a \in \mathcal{A}} Q_d^*(b, a) = \max_{a \in \mathcal{A}} \{R(b, a) + \gamma \mathbb{E}[V_{d+1}^*(ba)|b]\} \quad (37)$$

$$\hat{V}_d(b) \equiv \max_{a \in \mathcal{A}} \hat{Q}_d(b, a) = \max_{a \in \mathcal{A}} \{R(b, a) + \gamma \mathbb{E}[\hat{V}_{d+1}^{C_a}(ba)|b]\} \quad (38)$$

$$\hat{V}_d^{C_a}(b) \equiv \max_{a \in \text{VOO}(\mathcal{A}, C_a)} \hat{Q}_d(b, a) = \max_{a \in \text{VOO}(\mathcal{A}, C_a)} \{R(b, a) + \gamma \mathbb{E}[\hat{V}_{d+1}^{C_a}(ba)|b]\} \quad (39)$$

Repeating the procedures in Lemma 1, we closely follow the calculations from Lemma 5 in Kim et al. (2020):

$$\underbrace{|V_d^*(b) - \hat{V}_d(b)|}_{\text{VOO Recursive bound}} = \left| \max_{a \in \mathcal{A}} \{R(b, a) + \gamma \mathbb{E}[V_{d+1}^*(bao)|b]\} - \max_{a \in \mathcal{A}} \{R(b, a) + \gamma \mathbb{E}[\hat{V}_{d+1}^{C_a}(bao)|b]\} \right| \quad (40)$$

$$\leq \left| R(b, a^*) + \gamma \mathbb{E}[V_{d+1}^*(ba^*o)|b] - R(b, a^*) + \gamma \mathbb{E}[\hat{V}_{d+1}^{C_a}(ba^*o)|b] \right| \quad (a^* = \arg \max Q_d^*(b, a)) \quad (41)$$

$$\leq \gamma \mathbb{E} [|V_{d+1}^*(bao) - \hat{V}_{d+1}^{C_a}(bao)| |b|] \quad (42)$$

$$\leq \gamma \cdot \eta'(d+1) \quad (42)$$

$$\underbrace{|\hat{V}_d(b) - \hat{V}_d^{C_a}(b)|}_{\text{VOO Regret bound}} \leq \mathcal{R}_{C_a} \quad (43)$$

Thus, with our choice of C_a that is designed to satisfy the recurrence relation:

$$|V_d^*(b) - \hat{V}_d^{C_a}(b)| \leq \underbrace{|V_d^*(b) - \hat{V}_d(b)|}_{\text{VOO Recursive bound}} + \underbrace{|\hat{V}_d(b) - \hat{V}_d^{C_a}(b)|}_{\text{VOO Regret bound}} \quad (44)$$

$$\leq \gamma \cdot \eta'(d+1) + \mathcal{R}_{C_a} \leq \eta'(d) \quad (45)$$

(ii) POWSS Bound Similar to Lemma 1, the POWSS bound can also be further decomposed into the following terms:

$$|\hat{V}_d^{C_a}(b) - \tilde{V}_{\text{VOWSS},d}(b)| \leq \underbrace{|\hat{V}_d^{C_a}(b) - \tilde{V}_{\text{VOWSS},d}(b)|}_{\text{POWSS Concentration bound}} + \underbrace{|\tilde{V}_{\text{VOWSS},d}(b) - \hat{V}_{\text{VOWSS},d}(b)|}_{\text{POWSS Recursive bound}} \quad (46)$$

Here, the extra intermediate random variables are defined in the following manner (we omit denoting that the weighted averages for some belief bao and/or belief particle set \bar{ba} are conditioned upon appropriate b):

$$\tilde{V}_{\text{VOWSS},d}(b) \equiv \max_{a \in \text{VOO}(\mathcal{A}, C_a)} \tilde{Q}_{\text{VOWSS},d}(b, a) = \max_{a \in \text{VOO}(\mathcal{A}, C_a)} \left\{ \frac{\sum_{i=1}^{C_s} w_{d,i} (r_{d,i} + \gamma \hat{V}_{d+1}^{C_a}(bao_i))}{\sum_{i=1}^{C_s} w_{d,i}} \right\} \quad (47)$$

$$\hat{V}_{\text{VOWSS},d}(\bar{b}) \equiv \max_{a \in \text{VOO}(\mathcal{A}, C_a)} \hat{Q}_{\text{VOWSS},d}(\bar{b}, a) = \max_{a \in \text{VOO}(\mathcal{A}, C_a)} \left\{ \frac{\sum_{i=1}^{C_s} w_{d,i} (r_{d,i} + \gamma \hat{V}_{\text{VOWSS},d+1}(\bar{ba}o_i))}{\sum_{i=1}^{C_s} w_{d,i}} \right\} \quad (48)$$

Once again, we compare the two quantities by picking a reference action to directly compare the quantities inside the max operations. For the concentration bound term:

$$\underbrace{|\hat{V}_d^{C_a}(b) - \tilde{V}_{\text{VOWSS},d}(b)|}_{\text{POWSS Concentration bound}} \leq \left| \max_{a \in \text{VOO}(\mathcal{A}, C_a)} \{R(b, a) + \gamma \mathbb{E}[\hat{V}_{d+1}^{C_a}(bao)|b]\} \right. \quad (49)$$

$$\left. - \max_{a \in \text{VOO}(\mathcal{A}, C_a)} \left\{ \frac{\sum_{i=1}^{C_s} w_{d,i} (r_{d,i} + \gamma \hat{V}_{d+1}^{C_a}(bao_i))}{\sum_{i=1}^{C_s} w_{d,i}} \right\} \right| \quad (50)$$

$$\leq \left| R(b, a^*) + \gamma \mathbb{E}[\hat{V}_{d+1}^{C_a}(ba^*o)|b] - \frac{\sum_{i=1}^{C_s} w_{d,i} (r_{d,i} + \gamma \hat{V}_{d+1}^{C_a}(ba^*o_i))}{\sum_{i=1}^{C_s} w_{d,i}} \right| \quad (a^* = \arg \max_{V \in \text{VOO}} \hat{Q}_d(b, a))$$

Decomposing the quantity into the reward difference and the next-step value difference:

$$\underbrace{|\hat{V}_d^{C_a}(b) - \tilde{V}_{\text{VOWSS},d}(b)|}_{\text{POWSS Concentration bound}} \leq \underbrace{\left| R(b, a^*) - \frac{\sum_{i=1}^{C_s} w_{d,i} r_{d,i}}{\sum_{i=1}^{C_s} w_{d,i}} \right|}_{\text{Reward difference}} + \gamma \underbrace{\left| \mathbb{E}[\hat{V}_{d+1}^{C_a}(ba^*o)|b] - \frac{\sum_{i=1}^{C_s} w_{d,i} \hat{V}_{d+1}^{C_a}(ba^*o_i)}{\sum_{i=1}^{C_s} w_{d,i}} \right|}_{\text{Value difference}} \quad (51)$$

For the reward difference, we can crudely upper bound it by the POWSS Q -value estimate concentration bound in Theorem 2 of Lim, Tomlin, and Sunberg (2020), since this is effectively the same structure as the leaf node estimate. In the POWSS

concentration bound in Theorem 2, the difference has an upper bound of $\lambda/(1 - \gamma)$, which we will define as ϵ' , and we will refer to the exponentially decaying probability as p' . This bounds the quantity by $(\epsilon' + 2p' \cdot V_{\max})$ using the expectation version of the POWSS concentration bound.

$$\underbrace{\left| R(b, a^*) - \frac{\sum_{i=1}^{C_s} w_{d,i} r_{d,i}}{\sum_{i=1}^{C_s} w_{d,i}} \right|}_{\text{Reward difference}} \leq \epsilon' + 2p' \cdot V_{\max} \quad (52)$$

We could instead use Lemma 1 of Lim, Tomlin, and Sunberg (2020), the leaf node estimate concentration bound, but we use the more general Theorem 2 instead. This allows us to consistently use the same theorem throughout this analysis and we can effectively combine terms. Similarly, while the worst case bound is $2R_{\max}$ since we are taking the difference of two reward functions, we crudely upper bound that with $2V_{\max}$ for algebraic convenience of combining it with the value difference term.

$$\underbrace{\left| \mathbb{E}[\hat{V}_{d+1}^{C_a}(ba^*o)|b] - \frac{\sum_{i=1}^{C_s} w_{d,i} \hat{V}_{d+1}^{C_a}(ba^*o_i)}{\sum_{i=1}^{C_s} w_{d,i}} \right|}_{\text{Value difference}} \leq \epsilon' + 2p' \cdot V_{\max} \quad (53)$$

On the other hand, for the value difference, the POWSS concentration bound also turns out to be a crude upper bound, but with more sophisticated calculations. During this part of the proof, we will refer heavily back to the continued proof of Lemma 2 in the Appendix C of Lim, Tomlin, and Sunberg (2020) and give a general overview of how the steps apply here.

(ii)-a. Value Difference While Lemma 2 in Lim, Tomlin, and Sunberg (2020) is calculated with respect to the theoretically optimal value function V_{d+1}^* , the calculation steps themselves and the theorems and lemmas used there can apply exactly the same way for $\hat{V}_{d+1}^{C_a}$. We will briefly illustrate how the steps are parallel to the proof of Lemma 2 in the Appendix C of Lim, Tomlin, and Sunberg (2020).

The value difference corresponds to the difference between the expected value of $\hat{V}_{d+1}^{C_a}$ and the self-normalized importance sampling estimator of the expected value. This value difference specifically corresponds to the first two error terms in the continued proof of Lemma 2 in the Appendix C of Lim, Tomlin, and Sunberg (2020). The decomposition looks like the following:

$$\left| \mathbb{E}[\hat{V}_{d+1}^{C_a}(ba^*o)|b] - \frac{\sum_{i=1}^{C_s} w_{d,i} \hat{V}_{d+1}^{C_a}(ba^*o_i)}{\sum_{i=1}^{C_s} w_{d,i}} \right| \quad (54)$$

$$\leq \underbrace{\left| \mathbb{E}[\hat{V}_{d+1}^{C_a}(ba^*o)|b] - \frac{\sum_{i=1}^{C_s} w_{d,i} \hat{V}_{d+1}^{C_a}(s_{d,i}, b, a^*)}{\sum_{i=1}^{C_s} w_{d,i}} \right|}_{\text{Importance sampling error}} + \underbrace{\left| \frac{\sum_{i=1}^{C_s} w_{d,i} (\hat{V}_{d+1}^{C_a}(s_{d,i}, b, a^*) - \hat{V}_{d+1}^{C_a}(ba^*o_i))}{\sum_{i=1}^{C_s} w_{d,i}} \right|}_{\text{MC next-step integral approximation error}} \quad (55)$$

The next-step marginal integral $\hat{V}_{d+1}^{C_a}(s_{d,i}, b, a^*)$ is defined as:

$$\hat{V}_{d+1}^{C_a}(s_{d,i}, b, a^*) \equiv \int_S \int_O \hat{V}_{d+1}^{C_a}(ba^*o) \mathcal{Z}(o|a^*, s_{d+1}) \mathcal{T}(s_{d+1}|s_{d,i}, a^*) ds_{d+1} do \quad (56)$$

With this analogous definition, the self-normalized estimator identities in Lim, Tomlin, and Sunberg (2020) can be exactly applied to this setting once again, now instead for the function $\hat{V}_{d+1}^{C_a}$ because the algebraic steps taken in the proof should hold for our V function estimator as well. Intuitively, the next-step marginal integral is defined to be the marginal random variable for $\hat{V}_{d+1}^{C_a}$, instead of the optimal V function as it is done in the works of Lim, Tomlin, and Sunberg (2020).

First, following Lim, Tomlin, and Sunberg (2020), we define the following notation for products of transition and observation densities:

$$\mathcal{T}_{1:d}^i \equiv \prod_{n=1}^d \mathcal{T}(s_{n,i}|s_{n-1,i}, a_n) \quad (57)$$

$$\mathcal{Z}_{1:d}^{i,j} \equiv \prod_{n=1}^d \mathcal{Z}(o_{n,j}|a_n, s_{n,i}) \quad (58)$$

Specifically, i denotes the index of the state sample, and j denotes the index of the observation sample. Absence of any of the indices i or j means that the state trajectory $\{s_n\}$ and/or the observation history $\{o_n\}$ appear as regular variables, mostly for the purposes of integration.

(ii)-b. Importance Sampling Error For the importance sampling error, note that for a belief b at depth d ,

$$\mathbb{E}[\hat{V}_{d+1}^{C_a}(ba^*o)|b] = \int_S \int_S \int_O \hat{V}_{d+1}^{C_a}(ba^*o)(\mathcal{Z}_{d+1})(\mathcal{T}_{d,d+1})b \cdot ds_{d:d+1} do \quad (59)$$

$$= \int_S \hat{\mathbf{V}}_{d+1}^{C_a}(s_{d,i}, b, a^*)b \cdot ds_d \quad (60)$$

$$= \frac{\int_{S^d} \hat{\mathbf{V}}_{d+1}^{C_a}(s_{d,i}, b, a^*)(\mathcal{Z}_{1:d})(\mathcal{T}_{1:d})b_0 ds_{0:d}}{\int_{S^d} (\mathcal{Z}_{1:d})(\mathcal{T}_{1:d})b_0 ds_{0:d}} \quad (61)$$

Consequently, the weighted average of the next-step marginal integral $\hat{V}_{d+1}^{C_a}(s_{d,i}, b, a^*)$ is a self-normalized importance sampling estimator of $\hat{V}_{d+1}^{C_a}(ba^*o)$ given b , and we can apply the augmented self-normalized estimator concentration bound in the same way as Lim, Tomlin, and Sunberg (2020) to get the concentration bound of $\lambda/3$.

(ii)-c. Monte Carlo Next-Step Integral Approximation Error For the MC next-step integral approximation error, generating estimates of $\hat{V}_{d+1}^{C_a}(ba^*o_i)$ for a given $(s_{d,i}, b, a^*)$ also results in an unbiased Monte Carlo estimator of the next-step marginal integral, and the following difference is mean zero conditioned on $(s_{d,i}, b, a^*)$:

$$\Delta_{d+1}(s_{d,i}, b, a^*) \equiv \hat{\mathbf{V}}_{d+1}^{C_a}(s_{d,i}, b, a^*) - \hat{V}_{d+1}^{C_a}(ba^*o_i) \quad (62)$$

Thus, the same calculation steps hold. Note that in the works of Lim, Tomlin, and Sunberg (2020), the MC next-step integral approximation error is further crudely bound by $\frac{2}{3\gamma}\lambda$, when the actual bounds also hold for $\frac{2}{3}\lambda$, for the convenience of being able to combine the γ multiplied terms in the main proof of Lemma 2. Thus, we can bound the MC next-step integral approximation error with the stricter bound $\frac{2}{3}\lambda$.

In our work, we used the variable ϵ' to denote the POWSS concentration bound, which corresponds to $\epsilon' = \lambda/(1-\gamma) \geq \lambda$. Since the sum of importance sampling error and MC next-step integral approximation error are bounded by $(1/3 + 2/3)\lambda = \lambda$, this can also further be crudely bounded by the POWSS concentration inequality with the upper bound ϵ' .

We have now obtained bounds for the value difference term using the expectation version of the POWSS concentration inequality where the extreme probability event is once again bounded with the term $2p' \cdot V_{\max}$:

$$\left| \mathbb{E}[\hat{V}_{d+1}^{C_a}(ba^*o)|b] - \frac{\sum_{i=1}^{C_s} w_{d,i} \hat{V}_{d+1}^{C_a}(ba^*o_i)}{\sum_{i=1}^{C_s} w_{d,i}} \right| \leq \epsilon' + 2p' \cdot V_{\max} \quad (63)$$

Finally, we can bound the POWSS Concentration bound term:

$$\underbrace{\left| \hat{V}_d^{C_a}(b) - \tilde{V}_{\text{VOWSS},d}(b) \right|}_{\text{POWSS Concentration bound}} \leq (\epsilon' + 2p' \cdot V_{\max}) + \gamma(\epsilon' + 2p' \cdot V_{\max}) = (1 + \gamma)(\epsilon' + 2p' \cdot V_{\max}) \quad (64)$$

For the POWSS Recursive bound term, we proceed with the similar recursive calculation as SS Recursive bound term done in Lemma 1 by using the inductive hypothesis for step $d+1$:

$$\underbrace{\left| \tilde{V}_{\text{VOWSS},d}(b) - \tilde{V}_{\text{VOWSS},d}(\bar{b}) \right|}_{\text{POWSS Recursive bound}} \leq \left| \max_{a \in \text{VOO}(\mathcal{A}, C_a)} \left\{ \frac{\sum_{i=1}^{C_s} w_{d,i} (r_{d,i} + \gamma \hat{V}_{d+1}^{C_a}(ba^*o_i))}{\sum_{i=1}^{C_s} w_{d,i}} \right\} \right| \quad (65)$$

$$- \max_{a \in \text{VOO}(\mathcal{A}, C_a)} \left\{ \frac{\sum_{i=1}^{C_s} w_{d,i} (r_{d,i} + \gamma \hat{V}_{\text{VOWSS},d+1}(\bar{ba^*o_i}))}{\sum_{i=1}^{C_s} w_{d,i}} \right\} \quad (66)$$

$$\leq \left| \gamma \frac{\sum_{i=1}^{C_s} w_{d,i} (\hat{V}_{d+1}^{C_a}(ba^*o_i) - \hat{V}_{\text{VOWSS},d+1}(\bar{ba^*o_i}))}{\sum_{i=1}^{C_s} w_{d,i}} \right| \quad (\tilde{a} = \arg \max_{VOO} \tilde{Q}_{\text{VOWSS},d}(b, a)) \quad (67)$$

$$\leq \gamma \frac{\sum_{i=1}^{C_s} w_{d,i} \left| \hat{V}_{d+1}^{C_a}(ba^*o_i) - \hat{V}_{\text{VOWSS},d+1}(\bar{ba^*o_i}) \right|}{\sum_{i=1}^{C_s} w_{d,i}} \quad (68)$$

$$\leq \gamma \cdot \alpha'_{d+1}$$

Putting the POWSS components together, we prove the POWSS bound by induction:

$$\left| \hat{V}_d^{C_a}(b) - \hat{V}_{\text{VOWSS},d}(\bar{b}) \right| \leq \underbrace{\left| \hat{V}_d^{C_a}(b) - \tilde{V}_{\text{VOWSS},d}(b) \right|}_{\text{POWSS Concentration bound}} + \underbrace{\left| \tilde{V}_{\text{VOWSS},d}(b) - \hat{V}_{\text{VOWSS},d}(\bar{b}) \right|}_{\text{POWSS Recursive bound}} \quad (69)$$

$$\leq (1 + \gamma)(\epsilon' + 2p' \cdot V_{\max}) + \gamma \cdot \alpha'_{d+1} = \alpha'_d \blacksquare \quad (70)$$

Proof for Theorem 2. Finally, we prove the main theorem by combining the two terms:

$$\left| V_d^*(b) - \hat{V}_{\text{VOWSS},d}(\bar{b}) \right| \leq \underbrace{\left| V_d^*(b) - \hat{V}_d^{C_a}(b) \right|}_{\text{VOO bound}} + \underbrace{\left| \hat{V}_d^{C_a}(b) - \hat{V}_{\text{VOWSS},d}(b) \right|}_{\text{POWSS bound}} \leq \eta'(d) + \alpha'_d \leq \eta' + \alpha' \blacksquare \quad (71)$$

B Experiment Hyperparameters

Hyperparameters were taken from the references if they were given, and otherwise the set of hyperparameters for a system was obtained by first training POMCPOW, and then training VOMCPOW and BOMCP centered around POMCPOW parameters as initial estimates. This usually augmented the performances of VOMCPOW and BOMCP compared to directly borrowing the POMCPOW parameters. For BOMCP, buffer and k were fixed at 100 and 5, respectively, as it was done in the original paper by Mern et al. (2021b). Table 2 shows the final hyperparameters used in the experiments. Specifically for the lunar lander problem, we have chosen the dynamics time step $dt = 0.4$, which gave us the most consistent performance of BOMCP with 100 queries over 1000 iterations that is in line with the results of Mern et al. (2021b).

As noted in the main body of the paper, the only hyperparameter that was manually picked is the Gaussian covariance matrix for VOO rejection sampling. When picking this covariance matrix, we usually found that it was most effective to use a diagonal matrix with entries that are around 10 to 20 times less than the maximum action space bounds for each dimensions. In theory, the diagonal covariance matrix can also be fitted via CEM, but we chose to handpick these values after some inspection in order to reduce the number of hyperparameters that needed to be fit. We also capped the number of rejection sampling iterations to 20, as well as sometimes manually setting automatic sample acceptance regions depending on the system, which is not strictly necessary.

	LQG	VDP Tag	Lunar Lander
Max Depth	3	10	250
POMCPOW			
c	65.0	110.0	10.0
k_a	30.0	30.0	3.0
α_a	$\frac{1}{2.5}$	$\frac{1}{30}$	$\frac{1}{4}$
k_o	30.0	5.0	2.0
α_o	$\frac{1}{4}$	$\frac{1}{100}$	$\frac{1}{10}$
VOMCPOW			
c	60.0	85.0	30.0
k_a	25.0	30.0	4.0
α_a	$\frac{1}{5.5}$	$\frac{1}{30}$	$\frac{1}{4}$
k_o	25.0	2.5	1.5
α_o	$\frac{1}{2.5}$	$\frac{1}{100}$	$\frac{1}{5}$
p_{VOO}	0.8	0.7	0.9
$\text{diag}(\sigma_{VOO}^2)$	[0.5, 0.5]	[0.1]	[0.2, 0.5, 0.05]
BOMCP			
c	135.0	-	10.0
k_a	30.0	-	3.0
α_a	$\frac{1}{4}$	-	$\frac{1}{4}$
k_o	20.0	-	2.0
α_o	$\frac{1}{4}$	-	$\frac{1}{10}$
l	$\log(15)$	-	$\log(15)$
λ	0.4	-	0.5
VOWSS			
C_s	10	-	-
C_a	100	-	-
γ_a	0.4	-	-
p_{VOO}	0.8	-	-
$\text{diag}(\sigma_{VOO}^2)$	[0.5, 0.5]	-	-

Table 2: Summary of hyperparameters used in experiments for POMCPOW, VOMCPOW, BOMCP, and VOWSS.